










## Bone collagen from subtropical Australia is preserved for more than 50,000 years

Carli Peters <sup>1✉</sup>, Yiming Wang<sup>1</sup>, Vikram Vakil<sup>2</sup>, Jonathan Cramb<sup>2</sup>, Joe Dortch<sup>3</sup>, Scott Hocknull <sup>4,5</sup>, Rochelle Lawrence <sup>4</sup>, Tiina Manne<sup>1,6</sup>, Carly Monks<sup>3</sup>, Gertrud E. Rössner <sup>7,8</sup>, Helen Ryan<sup>9</sup>, Mikael Siversson<sup>9</sup>, Tim Ziegler <sup>10</sup>, Julien Louys <sup>11</sup>, Gilbert J. Price <sup>2</sup>, Nicole Boivin <sup>1,6,12</sup> & Matthew J. Collins <sup>13,14</sup>

Ancient protein studies have demonstrated their utility for looking at a wide range of evolutionary and historical questions. The majority of palaeoproteomics studies to date have been restricted to high latitudes with relatively temperate environments. A better understanding of protein preservation at lower latitudes is critical for disentangling the mechanisms involved in the deep-time survival of ancient proteins, and for broadening the geographical applicability of palaeoproteomics. In this study, we aim to assess the level of collagen preservation in the Australian fossil record. Collagen preservation was systematically examined using a combination of thermal age estimates, Fourier Transform Infrared Spectroscopy, Zooarchaeology by Mass Spectrometry, and protein deamidation calculations. We reveal unexpected subtropical survival of collagen in bones more than 50 thousand years old, showing that protein preservation can exceed chemical predictions of collagen survival in bone. These findings challenge preconceptions concerning the suitability of palaeoproteomics in subtropical Pleistocene environments. We explore potential causes of this unexpected result to identify the underlying mechanisms leading to this exceptional preservation. This study serves as a starting point for the analysis of ancient proteins in other (sub)tropical contexts, and at deeper timescales.

<sup>1</sup>Department of Archaeology, Max Planck Institute of Geoanthropology, Jena, Germany. <sup>2</sup>School of Earth and Environmental Sciences, The University of Queensland, Brisbane, QLD 4072, Australia. <sup>3</sup>School of Social Sciences, University of Western Australia, Perth, WA 6009, Australia. <sup>4</sup>Geosciences, Queensland Museum, Hendra, QLD 4011, Australia. <sup>5</sup>Faculty of Science, Monash University, Melbourne, VIC 3010, Australia. <sup>6</sup>School of Social Science, The University of Queensland, Brisbane, QLD 4071, Australia. <sup>7</sup>Staatliche Naturwissenschaftliche Sammlungen Bayerns – Bayerische Staatssammlung für Paläontologie und Geologie, Munich, Germany. <sup>8</sup>Department für Geo- und Umweltwissenschaften, Paläontologie & Geobiologie, Ludwig-Maximilians-Universität München, Munich, Germany. <sup>9</sup>Western Australian Museum, Collections and Research, Welshpool, WA 6106, Australia. <sup>10</sup>Museums Victoria Research Institute, Melbourne Museum, Carlton, VIC 3053, Australia. <sup>11</sup>Australian Research Centre for Human Evolution, Griffith University, Nathan, QLD 4111, Australia. <sup>12</sup>Griffith Sciences, Griffith University, Nathan, QLD 4111, Australia. <sup>13</sup>McDonald Institute for Archaeological Research, University of Cambridge, Cambridge, UK. <sup>14</sup>The Globe Institute, Faculty of Health and Medical Sciences, University of Copenhagen, Copenhagen, Denmark.

✉email: [peters@gea.mpg.de](mailto:peters@gea.mpg.de)

Ancient protein and ancient DNA (aDNA) analysis have become crucial tools for studying the archaeological record. Much early research focused on the high Arctic<sup>1,2</sup> where cold conditions slowed decay rates. Over time, research attention has expanded into lower latitudes<sup>3,4</sup>, and further back in time<sup>5–7</sup>. Nonetheless, biomolecular archaeological research in the (sub)tropics remains limited<sup>8–11</sup>.

Compared to aDNA, ancient proteins have higher preservation potential in harsh environments<sup>4,12,13</sup>. While proteins in tooth enamel or shell are trapped within minerals, bone protein is a mineralised composite connected to and influenced by the burial environment. Low pH will dissolve the bioapatite and expose the bone to biodegradation, whereas at neutral and higher pH, bioapatite is more stable and the extent of protein degradation will depend upon the chemical and environmental conditions of the burial context, including pH and site hydrology<sup>12,14–16</sup>. The preservation of proteins in the archaeological record can thus vary significantly between sites<sup>12,15,17</sup>. The oldest surviving peptide sequences were recovered from eggshell remains from north-western China dating to 6.5–9 Ma<sup>5</sup>. The oldest collagen peptides identified in the palaeontological record were extracted from high Arctic material dating back to 3.4 million years (Ma) ago<sup>2</sup>.

In closed systems like eggshell - in which pH and water availability are constrained - biomolecular decay is fairly predictable; it is this predictable decay (assuming a known thermal history) which enables amino acid racemization to work so successfully<sup>18–20</sup>. Attempts to predict protein survival<sup>21,22</sup> and degradation<sup>23</sup> in open systems, such as bone, are more challenging due to variations in water availability, pH, cations and anions, and small organic molecules which may be involved in cross-reactions, even in cases where there is no evidence of microbial activity. For example, it is possible to observe enhanced preservation in arid environments<sup>24</sup>, or accelerated decay as a result of alkaline conditions (e.g. bat guano in caves<sup>25</sup>). In the case of bone apatite, the mineral does not dissolve at alkaline pH, while both DNA and proteins undergo accelerated hydrolysis<sup>26</sup>. The predictive upper limit of collagen survival in bone<sup>14</sup> was thought to be robust, as evidenced by the development of models to predict the successful recovery of collagen for radiocarbon dating in temperate environments<sup>16</sup>. However, cases in which biomolecular preservation exceeds chemical predictions are far more intriguing<sup>6</sup>.

Previous studies on collagen degradation in ancient bone primarily focused on the temperate environments of Eurasia<sup>27–29</sup> and North America<sup>30</sup>. Few studies have explored collagen preservation in warmer and wetter environments that are presumed to be less favourable to the long-term preservation of biomolecules<sup>31</sup>. Here, we show that this is not the case in subtropical Australia.

This study systematically examines collagen survival in the Australian fossil record. Australia has an ideal setting to explore collagen preservation in fossils from challenging climatic and depositional contexts. The climatic conditions in Australia are highly variable, ranging from tropical conditions in the north to temperate conditions in the south. Depositional contexts in Australia range from open lacustrine and fluvial deposits through swampy, to cavernous deposits. These highly variable environments significantly affect the preservation potential of ancient biomolecules. However, the survival of biomolecules across the Australian archaeological and palaeontological record has not yet been quantitatively assessed, and for most regions biomolecular studies are lacking altogether.

We analyse fossil bone from Quaternary archaeological and palaeontological sites across Australia, including various regions and depositional environments (cave, fluvial, lacustrine, and swamp deposits). Thermal age estimates and chemical predictions are used to determine biomolecular preservation potential, while

visual taphonomic assessments and Fourier Transform Infrared Spectroscopy (FTIR) analyses evaluate bone preservation. Zooarchaeology by Mass Spectrometry (ZooMS) success rates and collagen deamidation rates serve as proxies for collagen preservation. The results are compared between sites and against site-specific burial-conditions that impact collagen survival. Our study demonstrates the extraction of ancient proteins from bones in subtropical Australian contexts dating back to the Late Pleistocene. These findings inform future studies and aid in assessing the potential for successful palaeoproteomics analysis of fossil material. Additionally, the study contributes to our understanding of collagen preservation in harsh environments over long timescales.

## Results

**Thermal age estimates.** Thermal age estimates were calculated for each locality using both a shallow and a deep model (Supplementary Methods, Table S2, Supplementary Data 5). The majority of the localities have thermal age estimates exceeding 200,000 years, even when using a more 'optimistic' deep model with lower thermal fluctuations. Some sites, including Robert Broom Cave and Tripot Cave in Broken River, have thermal ages even exceeding 1 million years, indicating minimal collagen preservation. Conversely, sites with thermal age estimates below 200,000 years, such as Beehive (Broken River), Devil's Lair, Kudjal Yolghah Cave, Lake Victoria, Lancefield Swamp, Mammoth Cave, Tight Entrance Cave, and Yellabidde Cave, are expected to exhibit better collagen preservation.

**ZooMS and deamidation.** In total, 167 samples had sufficient collagen preservation for taxonomic identification using ZooMS (Supplementary Data 6). High variability was observed in ZooMS success rates - the percentage of successfully analysed and identified ZooMS samples - between localities (Fig. 1, Table S3). There are several localities where no collagen was successfully extracted (Boodie Cave, Darling Downs, Lake Victoria, Morwell, South Walker Creek, and Strathdownie). Relatively good collagen preservation was observed at other sites, with Millennium Cave (Broken River) and Devil's Lair providing the highest overall success rates at 100% and 85%, respectively.

Deamidation rates were calculated for all samples that were successfully analysed with ZooMS. A deamidation value of 1 refers to a peptide that shows no evidence of deamidation, while a deamidation value of 0 indicates that the peptide is fully deamidated<sup>32</sup>. The resulting deamidation rates range between 0.16 and 0.99. The average deamidation rates varied from 0.17 to 0.95 (Table S3), indicating significant variability in collagen preservation across sites. Spring Creek exhibited the highest level of deamidation, while McEachern Cave showed the lowest level. Usefully, average deamidation rates show a high correlation (Pearson correlation coefficient ( $r$ ): 0.97) to ZooMS success rates (Fig. 2), although they do not correlate with the absolute and thermal ages of the sites, or with the FTIR results (Figure S3). This implies that with increasing deamidation, fewer peptides with taxonomic discrimination persist. This phenomenon should be explored further, as it would imply that deamidation is a useful index of likely success rate for ZooMS identifications. The results of this study support earlier claims that glutamine deamidation cannot be used reliably as a relative measure of time, but should rather be used as a measure of collagen preservation<sup>33–36</sup>.

**Method comparison.** No correlation was observed between thermal age estimates and ZooMS success rates. Sufficient collagen for relatively high ZooMS success rates (>35%) was recovered from both localities with relatively young thermal age

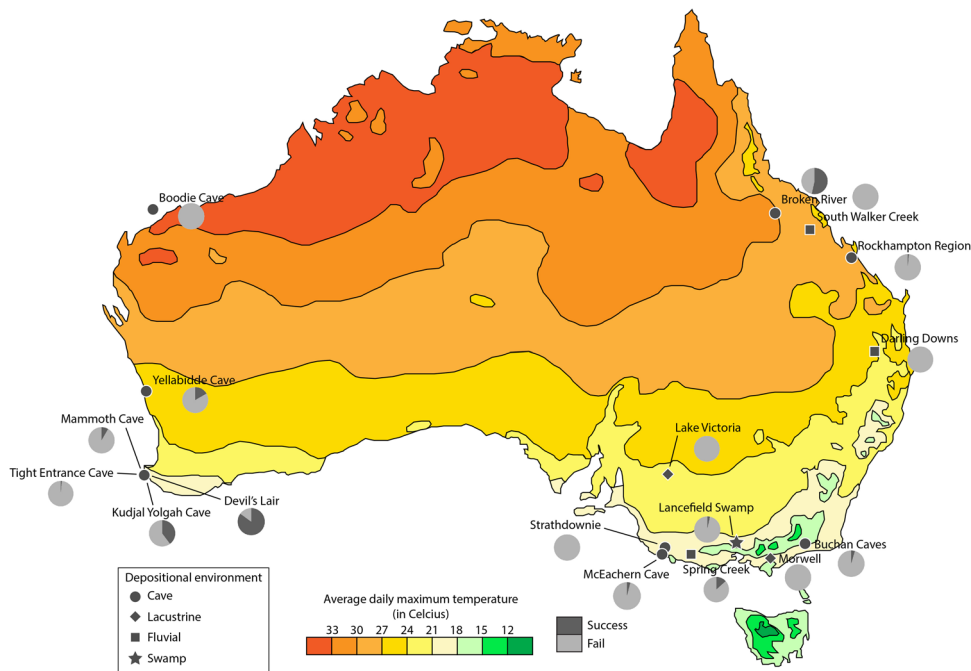


**Fig. 1 ZooMS success rates for each locality.** Dark grey: samples with sufficient collagen preservation to make a taxonomic identification with ZooMS. Light gray: samples with insufficient collagen preservation to make a taxonomic identification with ZooMS. Temperature data from Australian Government, Bureau of Meteorology (1961-1990) does not reflect the full thermal history of the localities but illustrated which sites lie within similar thermal ranges.

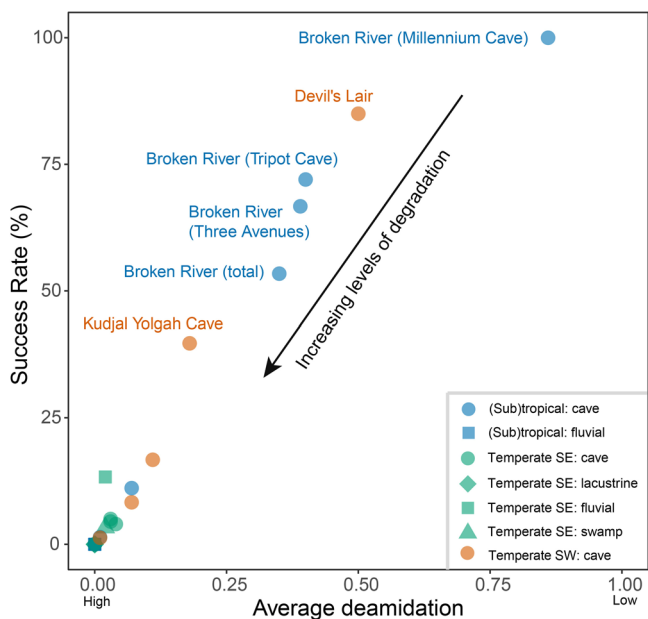


**Fig. 2 ZooMS success rates and average deamidation rates for each depositional environment by biogeographic zone.** Blue: (sub)tropical localities; green: localities in temperate southeast Australia; orange: localities in temperate southwest Australia. Circle: cave; square: fluvial deposit; diamond: lacustrine deposit; triangle: swamp deposit.

estimates as well as sites with old thermal age estimates forecasting a complete absence of collagen (Fig. 3). Similarly, localities with ZooMS success rates of <10% had thermal age estimates ranging from 52.3 to 6923.5 ka. Likewise, no correlation was observed between ZooMS success rates and bone weathering stages (following Behrensmeier<sup>37</sup>). Most moderately to heavily weathered bone samples preserved insufficient collagen to make

taxonomic identifications with ZooMS. Slightly more samples with milder weathering produced successful results (Figure S2). Overall, our results seem to indicate that bone weathering stages are a weak predictor of ZooMS success rates. However, the sample size for this group was too small to make reliable statistical inferences. These findings are consistent with the results of previous studies which demonstrated that the macroscopic appearance of bones is not a reliable indicator of collagen preservation for biomolecular analysis<sup>38</sup>.

A significant difference between samples with and without good collagen preservation was observed for Am1/P ( $t = -13.0$ ,  $df = 191.5$ ,  $p$  value < 0.001) and Am2/P ( $t = -12.2$ ,  $df = 198.2$ ,  $p$  value < 0.001) (Fig. 4). Our results provide important lessons in regard to the relationship between FTIR values and collagen preservation. In previous studies, FTIR cut-off points for Am1/P of >0.02<sup>38</sup> and >0.04<sup>39</sup> have been suggested to eliminate samples without sufficient collagen preservation for subsequent ZooMS analysis. However, for our sample set, these proposed cut-off points would also eliminate a large number of samples that actually had sufficient collagen preservation for ZooMS. Instead, a cut-off point for Am1/P of >0.05 would agree better with our dataset, even though this would still result in the loss of 20.6% of the successful samples. These findings indicate that suggested FTIR cut-off points should be used with caution, and evaluated in light of sample value and availability, and the particular research questions that are being addressed. In the light of the unexpectedly good preservation of collagen at the Australian sites studied here, the use of FTIR or other methods, such as near infrared spectroscopy (NIR)<sup>17,40</sup>, would seem worthwhile in studies of (sub)tropical bone material.

**Discussion**

**Regional differences in collagen preservation.** Localities analysed in this study were grouped into three regions reflecting their biogeographic zoning ((sub)tropical, temperate southeast, and temperate southwest) to investigate regional differences in preservation potential. The lowest levels of collagen survival were

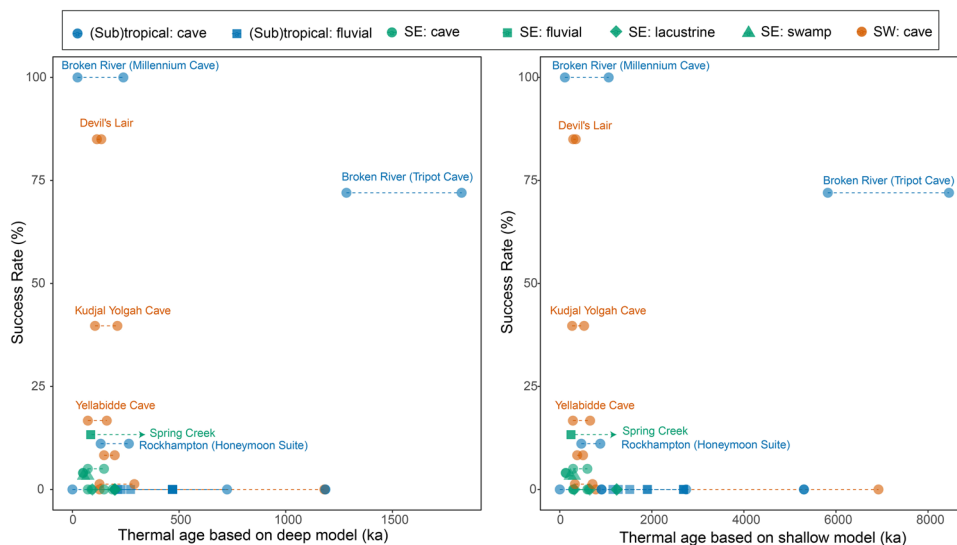


**Fig. 3 Comparison between thermal age estimates and ZooMS success rates.** Left panel: thermal age estimates based on deep model. Right panel: thermal age estimates based on shallow model. Blue: (sub)tropical localities; green: localities in temperate southeast Australia; orange: localities in temperate southwest Australia. Circle: cave; square: fluvial deposit; diamond: lacustrine deposit; triangle: swamp deposit.

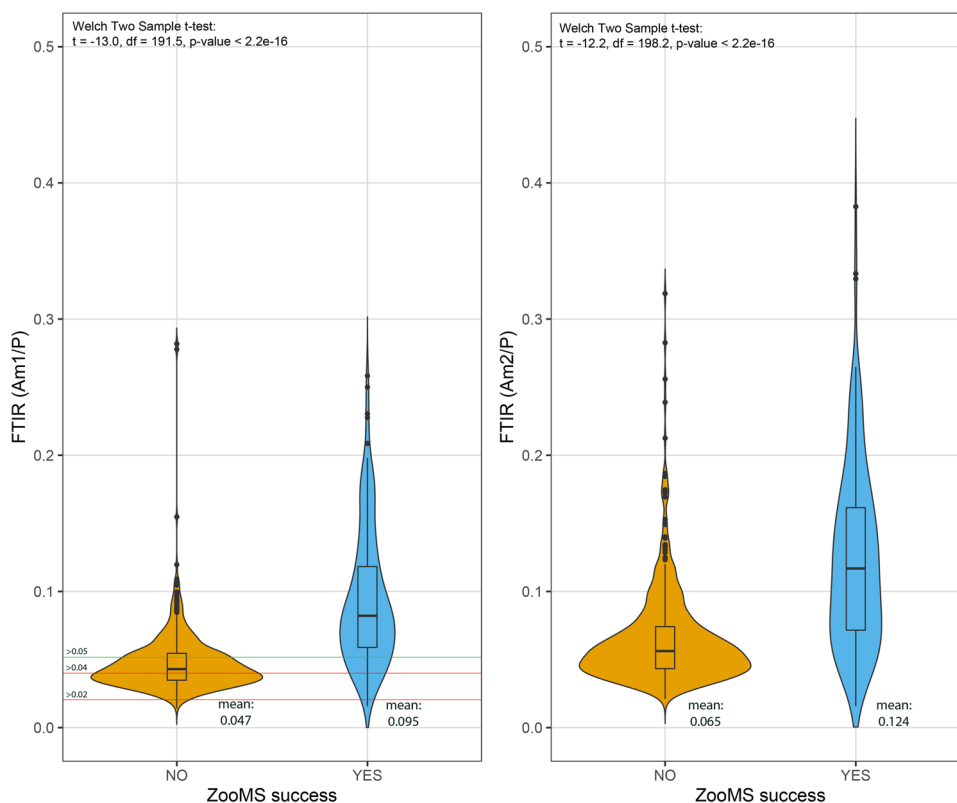


**Fig. 4 Violin plot showing the distribution of Am1/P and Am2/P values for samples with ( $n = 162$ ) and without ( $n = 486$ ) successful ZooMS results.** Mean values are indicated. The results of the t-test, indicating that these two distributions differ significantly, are shown in the top right. Horizontal green line indicated the cut-off point proposed in this study. Horizontal red lines indicate previously proposed cut-off points for Am1/P at  $>0.02$ <sup>38</sup> and  $>0.04$ <sup>39</sup>.

found at sites sampled from temperate SE Australia (Fig. 2), while sampled sites from subtropical to tropical regions provided higher levels of collagen preservation. In addition to the thermal history of a site, other micro-environmental factors such as soil pH<sup>15</sup>, hydrology<sup>16,29</sup>, and microbial activity<sup>41–43</sup>, can also influence the speed of collagen degradation (Supplementary Discussion 2). A combination of these factors could thus possibly explain the lack of collagen preservation at fossil sites in temperate SE Australia.

Further, the localities from temperate SE Australia reflect a wider variety of burial environments and a larger number of open-air sites. Open-air sites experience more extreme temperature fluctuations than cave sites, and bone material therein commonly exhibits higher rates of cracking and exposure, due to more frequent wet-dry cycles<sup>37</sup>. These additional factors could explain the low levels of collagen preservation observed at the temperate SE Australian sites included in the study.



### Depositional environment as an indicator of collagen survival.

Depositional environment plays an important role in the preservation of collagen in Australia. Caves have the highest overall ZooMS success rates in all regions of Australia (Fig. S4), although it has to be mentioned that only a limited number of lacustrine and swamp deposits was evaluated in this study which could bias the results. Overall, collagen preservation was best when fossil material was protected; in caves, the highest levels of collagen preservation came from deposits that were associated with capping flowstones, or when the deposit was distal to large open entrances with little to no root/insect activity (Table S1). Deposits that failed to yield collagen were also the most open cave systems included in the analysis, with significantly large entrances proximal to the bone deposits.

At open-air sites, carbonate-rich depositional environments, such as spring and tufa formations, yielded the highest levels of collagen preservation. Limestone caves were more favourable to the long-term preservation of bone collagen than acidic burial environments. The limited movement of water, and oversaturation of groundwater with carbonate in limestone caves and springs could further increase the potential for collagen preservation in these environments. In addition, the precise geochemical conditions of the depositional environment also likely play an important role in the survival of collagen, as this has also been shown to have a considerable impact on the diagenetic pathway of bone mineral<sup>44–46</sup>.

**Collagen preservation at Tripot Cave (Broken River).** In the Middle-Late Pleistocene deposit at Tripot Cave situated in the subtropical Broken River limestone karst area, the exceptional preservation of bone collagen far exceeds chemical predictions of collagen survival<sup>47</sup>. Whilst the recovery of Pleistocene-aged collagen is common from high latitudes, survival in subtropical settings has not been previously supported.

The high ZooMS success rates at Tripot Cave indicate that collagen at the site preserves much better than would be expected based upon previous predictions of collagen survival<sup>47</sup>. These predictions, based upon temperature dependence of the rate of gelatinisation of bone, appear to successfully identify a causal relationship between local environmental temperatures and limits to radiocarbon dating from bone collagen<sup>16</sup>. Other micro-environmental factors that impact collagen preservation such as soil hydrology and pH, are not included in thermal age calculations, which instead rely solely on assessments of age and temperature. However, all of these factors, except for extreme aridity, will retard hydrolysis<sup>48,49</sup>. They thus offer explanations only as to why collagen will *not* persist. There are uncertainties in estimating the thermal history of bone at Tripot Cave, and more generally, including: i) annual temperature fluctuations within the burial environment; ii) the quality of the palaeoclimate model; iii) the effect of burial depth; and iv) uncertainties in age estimates. However, with the exception of the latter, none of the other factors could offer sufficient uncertainty to explain the data from Tripot Cave. The failure of the model to predict the preservation of collagen thus highlights the limits of our understanding of the mechanisms of bone collagen degradation, and at the same time shows that thermal age models in their current form are not sufficient to predict preservation.

The preservation of collagen would be in line with chemical predictions of collagen preservation at the site if the bones were of Holocene age. The samples from this site come from the 'Left Wing', Units 1 and 2. Speleothems (indurated capping crust, interbedded flowstones, and flowstone clasts) in association with these two strata were dated with U-Th methods (Supplementary Discussion 1). Unit 2 has a poorly constrained maximum age

( $356 \pm 113$  thousand years (ka), corrected), and a minimum age of  $352 \pm 11$  ka. The maximum age of Unit 1 is constrained by the minimum age of Unit 2. An indurated calcite cap ( $73.2 \pm 3.5$  ka) constrains the minimum age of Unit 1. Unit 1 is likely to be close in age to Unit 2 given the similarities in lithology and faunal diversity, including proportion of extinct taxa, recovered. The chronology of the Tripot Cave deposits thus does not provide an explanation for the exceptional collagen preservation observed.

A possible explanation for the preservation of collagen at Tripot Cave could come from the polymer-in-a-box model<sup>50</sup>. As collagen degrades, the fibrils shorten and undergo radial expansion which, if constrained, will result in stabilisation of collagen fibrils. The intimate association of collagen with bone mineral<sup>51</sup> will inhibit degradation of the fibrils, but once the mineral starts to degrade, collagen follows<sup>52</sup>. The persistence of this intimate association, perhaps bolstered by secondary carbonate at Tripot Cave, might explain the exceptional preservation of collagen. Experimentally determined rates of collagen loss from bone were conducted in water initially undersaturated with respect to carbonate and phosphate. Therefore, environments which promote the stabilisation of the nanocrystalline apatite<sup>51</sup> might reasonably stabilise the 'box' around the polymer and enhance the stability of the collagen fibril. To further investigate this possibility, carbonate to phosphate (C/P) ratios were calculated from the FTIR spectra (Fig. S5). Modern bones have a C/P value of about 0.25<sup>53</sup>. The presence of calcite can lead to higher C/P values in archaeological bone, while lower C/P values indicate the loss of carbonate<sup>29</sup>. Australian sites with high ZooMS success rates had relatively high C/P values, indicating a high concentration of carbonates in the bones. Interestingly, a similar correlation has been observed between C/P ratio and DNA preservation<sup>54</sup>. However, when looking at C/P values of individual specimens from Tripot Cave, there does not appear to be a correlation between collagen preservation and C/P ratios (Fig. S6).

There is only minor development of speleothems in Tripot Cave. In the absence of large amounts of calcium carbonate moving through the cave chamber it is most likely that another mineral present is responsible for the remineralization process. For example, in leather tanning, chromium(III) has been shown to be able to form a matrix that is tightly bound to collagen, increasing the hydrothermal stability of the collagen<sup>52</sup>. Interestingly, it has previously been shown that the absence of calcium carbonate from tropical limestone cave systems can lead to the exceptional preservation of organic material as diagenesis alters the crystallinity and ordering of the bone mineral. Here, other ions, such as sodium, fluorine, and strontium, are involved in the remineralization process<sup>44</sup>. Unfortunately, detailed information about the geochemistry of Tripot Cave is currently unavailable, and it is not yet possible to disentangle which minerals are moving through the cave system leading to the exceptional preservation of collagen at the site.

**Future prospects.** This study has shown that it is possible to successfully extract collagen from Australian fossil material >50 ka old from apparently less than ideal preservation conditions, pushing back the limit of collagen preservation in subtropical latitudes. It also raises further questions about the potential preservation of ancient biomolecules in other environments that were previously deemed unfavourable. The preservation of collagen in the archaeological and palaeontological record of Australia does not seem to follow one given pattern, but instead appears to be dependent on site-specific burial environments and environmental conditions in addition to more recognised factors such as age, temperature and humidity, as has also been shown to be the case

for other regions in the world<sup>29,43–45,55</sup>. This also highlights the need for a critical re-examination of thermal age as an approach to predict collagen survival. Instead, approaches like NIR which can non-destructively assess the level of collagen preservation in a bone<sup>17,40</sup>, may become increasingly important in the future.

Whilst it is fairly easy to explain instances in which collagen yield is lower than predicted on the basis of a crude model, it is much more difficult to explain the opposite. There are only a few circumstances, such as extreme aridity, in which collagen survival is underestimated by the model. The fact that collagen is persisting in subtropical sites well beyond the limit of prediction is remarkable and offers the prospect that the application of palaeoproteomics may be extended far beyond its current scope. At the same time, this study highlights our limited understanding of the processes that act to reduce protein degradation. Tripot Cave offers a unique opportunity to study these processes in greater detail to understand the mechanisms behind protein preservation and identify other potential sites of exceptional preservation. Also important will be continued exploration of protein preservation across a wider range of (sub)tropical and other seemingly ‘unpromising’ sites to further test preservation concepts. Our results demonstrate that mechanisms of protein survival will not be fully elucidated if research remains focused primarily on high latitude and temperate environment sites. Finally, it is noteworthy that estimated temperature dependence upon collagen loss in bone is much higher than equivalent estimates of the rate of DNA depurination<sup>56</sup>. This also means that as temperatures increase, the rate of collagen degradation is estimated to accelerate more than DNA. The perception that bone collagen survives much longer than DNA, which is based on studies from temperate settings, thus may no longer hold true for contexts with high temperature extremes and could enhance the possibility of finding aDNA in these contexts.

## Materials and methods

**Material.** Seventeen localities ranging from north-eastern to south-western Australia, ranging in age from recent to the Late-Middle Pleistocene were included in this study (Table S1). The localities represent a wide range of depositional environments and environmental conditions. The depositional environment for each locality was categorised as either *cave*, *fluvial*, *lacustrine*, or *swamp*, and for each locality data was collected about the age of the fossils, burial environment, soil type, and pH (Supplementary Data 1). In total, 765 bone fragments were included in this study (Supplementary Data 2).

## Methods

**Thermal age estimates.** Past and present climate data were used to calculate thermal age estimates for collagen for each locality. Present-day mean annual temperature (MAT), mean monthly temperature, and mean annual precipitation data was collected from local weather stations in the vicinity of the localities (Supplementary Data 3). Palaeoclimate estimates were extracted from a statistically-derived high-resolution dataset of global terrestrial climate, bioclimate and vegetation of the last 120 kyr<sup>57</sup>. MAT (BIO01), maximum annual temperature (BIO05), minimum annual temperature (BIO06), annual temperature range (BIO07), annual precipitation (BIO12), and altitude data was extracted from the dataset with R v.4.0.1. with R Studio v.1.2.1717<sup>58</sup> using the Pastclim package v. 0.9.0<sup>59</sup>. These variables were collected for each locality in a time-series of 1000-year intervals up to a maximum of 100 kyr (Supplementary Data 4). Modern weather station data was compared to palaeoclimate estimates to verify the accuracy of the palaeoclimatic reconstruction. This comparison shows that the predicted temperatures based on the palaeoclimate

reconstructions are in line with what would be expected based on modern local temperature conditions (Figure S1).

Present-day altitudes of the localities have been estimated from (<https://www.advancedconverter.com/map-tools/find-altitude-by-coordinates>) and were used to correct for altitude differences between the localities, nearby weather stations, and the raster tiles of the palaeoclimate dataset. To account for differences in burial depth between localities, two models were used to calculate thermal age estimates for each locality: a shallow model, and a deep model<sup>60</sup>. For the shallow model, it was assumed that fossil material was deposited just below the surface meaning that temperature fluctuates throughout the year, while for the deep model it was assumed that fossil material was situated at a deeper burial depth. Here, the overlying sediments would have acted as a buffer against surface temperature changes at the surface. Therefore, temperature was assumed to remain stable all-year-round.

**Taphonomic assessment.** All bone fragments included in the analysis were subjected to visual taphonomic assessment prior to sampling for destructive analysis. All bones were photographed, and the colour of each fragment was documented. Bone weathering stages were also recorded for each fragment following the weathering stages outlined by Behrensmeyer<sup>37</sup>. Following this scale, a bone with weathering stage 0 shows no signs of weathering, whereas a bone with weathering stage 5 is completely falling apart.

**Fourier Transform Infrared Spectroscopy (FTIR).** FTIR is a minimally destructive technique that can be used to rapidly assess the preservation state of osseous remains (Supplementary Methods). FTIR analysis was carried out using a handheld FTIR (4300 Handheld, Agilent Technologies) with an attenuated total reflectance (ATR) diamond. One to two mg of bone powder from each sample was used for FTIR analysis and pressed against the ATR diamond to measure absorbance spectra with a spectral range of 2000–650  $\text{cm}^{-1}$ , a resolution of 4  $\text{cm}^{-1}$ , and 32 sample scans. Background measurements were taken between every sample. Resulting absorbance spectra were analysed using the MicroLab PC software package v. 5.2.1748.0 (Agilent Technologies). The height of the phosphate  $\nu_3$  ( $\sim 1035/1010 \text{ cm}^{-1}$ ), carbonate ( $\sim 1415 \text{ cm}^{-1}$ ), Amide I ( $\sim 1650 \text{ cm}^{-1}$ ), and Amide II ( $\sim 1550 \text{ cm}^{-1}$ ) absorption peaks were recorded. These were used to calculate the Amide I to phosphate ratio (Am1/P), the Amide II to phosphate (Am2/P) ratio, and the carbonate to phosphate (C/P) ratio.

**Zooarchaeology by Mass Spectrometry (ZooMS).** Collagen was extracted from fossil bone samples alongside extraction blanks following an acid-soluble approach adapted from previously published methods<sup>13,61</sup>. 50–70 mg of bone powder was demineralised in 400  $\mu\text{l}$  of 0.6 M hydrochloric acid (HCl) for 5 days. The samples were heated for 30 min at 65 °C, after which the supernatant was transferred to a 10 kDa ultrafilter (Microcon, Merck Millipore<sup>®</sup>) and centrifuged until completely passed through the filter. The samples were washed two times by adding 300  $\mu\text{l}$  of 50 mM ammonium bicarbonate (AmBic) to the ultrafilter and centrifuging until completely passed through the filter. The fraction that did not pass through the filter was resuspended in 100  $\mu\text{l}$  of 50 mM AmBic and digested on the filter with 1  $\mu\text{l}$  of 0.4  $\mu\text{g} \mu\text{l}^{-1}$  trypsin solution (Pierce™ Trypsin Protease, Thermo Scientific) for 18 h at 37 °C. Subsequent to enzymatic digestion, the samples were centrifuged a final time until completely passed through the filter. Peptides were purified and concentrated using C18 ZipTips (Pierce™ C18 Tips, Thermo Scientific).

Samples were spotted in duplicate onto an MTP Groundsteel 384-target plate, together with matrix solution ( $\alpha$ -cyano-4-hydroxycinnamic acid of 10  $\text{mg ml}^{-1}$  in 50% acetonitrile (ACN)/0.1% trifluoroacetic acid (TFA)). Samples were analysed

using an Autoflex Speed LRF matrix-assisted laser desorption/ionisation time of flight mass spectrometer (MALDI-TOF-MS, Bruker Daltonics) with a smartbeam-II laser. A SNAP averaging algorithm was used to obtain monoisotopic masses (C: 4.9384, N: 1.3577, O: 1.4773, S: 0.00417, H: 7.7583). Resulting MALDI spectra were visually inspected using FlexAnalysis v. 3.4 (Bruker Daltonics) and compared to a reference database consisting of published peptide markers for Australian taxa<sup>62,63</sup>.

**Deamidation.** Levels of glutamine deamidation were calculated from MALDI spectral data in R v.4.0.1. with R Studio v.1.2.1717<sup>58</sup> using the Q2E package<sup>32</sup>. This resulted in a quality score (%Gln) between 0–1 for all spectra, in which a quality score of 0 represents a fully deamidated peptide, and a quality score of 1 represents a peptide that shows no sign of deamidation<sup>32</sup>. Deamidation rates were only calculated for samples that could be taxonomically identified to family-level or higher taxonomic precision using ZooMS. Samples with insufficient collagen preservation for taxonomic identification were given a deamidation score of 0 for statistical analysis, representing the absence of measurable collagen in the sample.

**Statistics.** All statistical analyses were performed in R v.4.0.1. with R Studio v.1.2.1717<sup>58</sup>. To test whether FTIR values (Am1/P and Am2/P) can predict the success of ZooMS extractions, violin plots were used to show whether the FTIR value distributions for samples that were successfully and unsuccessfully analysed with ZooMS differed. Student t-tests were performed to assess whether there were significant differences in FTIR values between failed and successful ZooMS samples. A Pearson correlation coefficient ( $r$ ) was used to assess the correlation between ZooMS success rates and average deamidation rates. Unless otherwise stated, statistical significance was assessed at  $p < 0.01$ . A cut-off point was determined by calculating the third quantile of the failed samples. Clustered heatmaps were rendered to visualise variations in meteorological conditions between sites and reveal hierarchical clusters – a two-way display of a data-matrix in which the colour of a cell is proportional to its position along a colour gradient. Because the variables in the matrix are highly divergent, each variable column was normalised for the cluster algorithms. The dendrogram on the heatmap computes the distance between each pair of rows and columns, and orders them by similarity. The length of the branches on the heatmap represents the Euclidean distance, or dissimilarity, between clusters. Figures were made using the “ggplot2” package<sup>64</sup>.

**Reporting summary.** Further information on research design is available in the Nature Portfolio Reporting Summary linked to this article.

### Data availability

MALDI-Tof-MS spectra are publicly available via Zenodo (<https://doi.org/10.5281/zenodo.7825351>)<sup>65</sup>.

Received: 4 August 2023; Accepted: 15 November 2023;

Published online: 25 November 2023

### References

1. Miller, W. et al. Sequencing the nuclear genome of the extinct woolly mammoth. *Nature* **456**, 387–390 (2008).
2. Ryczynski, N. et al. Mid-Pliocene warm-period deposits in the High Arctic yield insight into camel evolution. *Nat. Commun.* **4**, 1–9 (2013).
3. Chen, F. et al. A late Middle Pleistocene Denisovan mandible from the Tibetan Plateau. *Nature* **569**, 409–412 (2019).
4. Cappellini, E. et al. Early Pleistocene enamel proteome from Dmanisi resolves *Stephanorhinus* phylogeny. *Nature* **574**, 103–107 (2019).
5. Demarchi, B. et al. Survival of mineral-bound peptides into the Miocene. *eLife* **11**, e82849 (2022).
6. Slon, V. et al. Extended longevity of DNA preservation in Levantine Paleolithic sediments, Sefunim Cave, Israel. *Sci. Rep.* **12**, 14528 (2022).
7. Kjær, K. H. et al. A 2-million-year-old ecosystem in Greenland uncovered by environmental DNA. *Nature* **612**, 283–291 (2022).
8. Welker, F. et al. Enamel proteome shows that *Gigantopithecus* was an early diverging pongine. *Nature* **576**, 262–265 (2019).
9. Demeter, F. et al. A Middle Pleistocene Denisovan molar from the Annamite Chain of northern Laos. *Nat. Commun.* **13**, 2557 (2022).
10. Buckley, M. et al. Archaeological collagen fingerprinting in the Neotropics: protein survival in 6000 year old dwarf deer remains from Pedro González Island, Pearl Islands, Panama in *Zooarchaeology in the Neotropics: Environmental diversity and human-animal interactions*, M. Mondini, A. Muñoz, & P. Fernández, Eds. (Springer, Cham), pp 157–175. (2017).
11. Harvey, V. L. et al. Interpreting the historical terrestrial vertebrate biodiversity of Cayman Brac (Greater Antilles, Caribbean) through collagen fingerprinting. *Holocene* **29**, 531–542 (2019).
12. Demarchi, B. et al. Protein sequences bound to mineral surfaces persist into deep time. *eLife* **5**, e17092 (2016).
13. Buckley, M., Collins, M., Thomas-Oates, J. & Wilson, J. C. Species identification by analysis of bone collagen using matrix-assisted laser desorption/ionisation time-of-flight mass spectrometry. *Rapid Commun. Mass Spectrom.* **23**, 3843–3854 (2009).
14. Smith, C. I., Chamberlain, A. T., Riley, M. S., Stringer, C. & Collins, M. J. The thermal history of human fossils and the likelihood of successful DNA amplification. *J. Hum. Evol.* **45**, 203–217 (2003).
15. Collins, M. et al. The survival of organic matter in bone: a review. *Archaeometry* **44**, 383–394 (2002).
16. Kendall, C., Eriksen, A. M. H., Kontopoulos, I., Collins, M. J. & Turner-Walker, G. Diagenesis of archaeological bone and tooth. *Palaeogeogr. Palaeoclimatol. Palaeoecol.* **491**, 21–37 (2018).
17. Sponheimer, M. et al. Saving old bones: a non-destructive method for bone collagen prescreening. *Sci. Rep.* **9**, 13928 (2019).
18. Dickinson, M. R., Lister, A. M. & Penkman, K. E. H. A new method for enamel amino acid racemization dating: a closed system approach. *Quat. Geochronol.* **50**, 29–46 (2019).
19. Tesakov, A. S. et al. Aminostratigraphical test of the East European Mammal Zonation for the late Neogene and Quaternary. *Quat. Sci. Rev.* **245**, 106434 (2020).
20. Penkman, K. E. H. et al. An aminostratigraphy for the British Quaternary based on Bithynia opercula. *Quat. Sci. Rev.* **61**, 111–134 (2013).
21. Allentoft, M. E. et al. The half-life of DNA in bone: measuring decay kinetics in 158 dated fossils. *Proc. Royal Soc. B. Biol. Sci.* **279**, 4724–4733 (2012).
22. Kistler, L., Ware, R., Smith, O., Collins, M. & Allaby, R. G. A new model for ancient DNA decay based on paleogenomic meta-analysis. *Nucleic Acids Res.* **45**, 6310–6320 (2017).
23. Van Doorn, N. L., Wilson, J. C., Hollund, H. I., Soressi, M. & Collins, M. Site-specific deamidation of glutamine: a new marker of bone collagen deterioration. *Rapid Commun. Mass Spectrom.* **26**, 2319–2327 (2012).
24. Shevchenko, A. et al. Proteomics identifies the composition and manufacturing recipe of the 2500-year old sourdough bread from Subeixi cemetery in China. *J. Prot.* **105**, 363–371 (2014).
25. Shahack-Gross, R., Berna, F., Karkanas, P. & Weiner, S. Bat guano and preservation of archaeological remains in cave sites. *J. Archaeol. Sci.* **31**, 1259–1272 (2004).
26. Collins, M. J., Riley, M. S., Child, A. M. & Turner-Walker, G. A basic mathematical simulation of the chemical degradation of ancient collagen. *J. Archaeol. Sci.* **22**, 175–183 (1995).
27. Matthiesen, H., Høier Eriksen, A. M., Hollesen, J. & Collins, M. Bone degradation at five Arctic archaeological sites: quantifying the importance of burial environment and bone characteristics. *J. Archaeol. Sci.* **125**, 105296 (2021).
28. Eriksen, A. M. H. et al. Rapid loss of endogenous DNA in pig bone buried in five different environments. *Archaeometry* **62**, 827–846 (2020).
29. Nielsen-Marsh, C. M. & Hedges, R. E. M. Patterns of diagenesis in bone I: the effects of site environments. *J. Archaeol. Sci.* **27**, 1139–1150 (2000).
30. Colleary, C., Lamadrid, H. M., O’Reilly, S. S., Dolocan, A. & Nesbitt, S. J. Molecular preservation in mammoth bone and variation based on burial environment. *Sci. Rep.* **11**, 2662 (2021).
31. Pestle, W. J. & Colvard, M. Bone collagen preservation in the tropics: a case study from ancient Puerto Rico. *J. Archaeol. Sci.* **39**, 2079–2090 (2012).
32. Wilson, J. C., Van Doorn, N. L. & Collins, M. Assessing the extent of bone degradation using glutamine deamidation in collagen. *Anal. Chem.* **84**, 9041–9048 (2012).



33. Brown, S. et al. Examining collagen preservation through glutamine deamidation at Denisova Cave. *J. Archaeol. Sci.* **133**, 105454 (2021).
34. Ramsøe, A. et al. DeamiDATE 1.0: Site-specific deamidation as a tool to assess authenticity of members of ancient proteomes. *J. Archaeol. Sci.* **115**, 105080 (2020).
35. Schroeter, E. R. & Cleland, T. P. Glutamine deamidation: an indicator of antiquity, or preservational quality? *Rapid Commun. Mass Spectrom.* **30**, 251–255 (2016).
36. Pal Chowdhury, M. et al. Collagen deamidation in archaeological bone as an assessment for relative decay rates. *Archaeometry* **61**, 1382–1398 (2019).
37. Behrensmeyer, A. K. Taphonomic and ecologic information from bone weathering. *Paleobiology* **4**, 150–162 (1978).
38. Kontopoulos, I. et al. Screening archaeological bone for palaeogenetic and palaeoproteomic studies. *PLoS ONE* **15**, e0235146 (2020).
39. Pothier Bouchard, G. et al. Portable FTIR for on-site screening of archaeological bone intended for ZooMS collagen fingerprint analysis. *J. Archaeol. Sci. Rep.* **26**, 101862 (2019).
40. Lugli, F. et al. Near-infrared hyperspectral imaging (NIR-HSI) and normalized difference image (NDI) data processing: an advanced method to map collagen in archaeological bones. *Talanta* **226**, 122126 (2021).
41. Hedges, R. E. M. Bone diagenesis: an overview of processes. *Archaeometry* **44**, 319–328 (2002).
42. Jans, M. M. E., Nielsen-Marsh, C. M., Smith, C. I., Collins, M. J. & Kars, H. Characterisation of microbial attack on archaeological bone. *J. Archaeol. Sci.* **31**, 87–95 (2004).
43. Fernández-Jalvo, Y. et al. Early bone diagenesis in temperate environments. Part I: surface features and histology. *Palaeogeogr. Palaeoclimatol. Palaeoecol.* **288**, 62–81 (2010).
44. de Sousa, D. V., Eltink, E., Oliveira, R. A. P., Félix, J. F. & Guimarães, Ld. M. Diagenetic processes in Quaternary fossil bones from tropical limestone caves. *Sci. Rep.* **10**, 21425 (2020).
45. Weiner, S., Goldberg, P. & Bar-Yosef, O. Three-dimensional distribution of minerals in the sediments of Hayonim Cave, Israel: diagenetic processes and archaeological implications. *J. Archaeol. Sci.* **29**, 1289–1308 (2002).
46. Thomas, D. B., Fordyce, R. E., Frew, R. D. & Gordon, K. C. A rapid, non-destructive method of detecting diagenetic alteration in fossil bone using Raman spectroscopy. *J. Raman Spectrosc.* **38**, 1533–1537 (2007).
47. Buckley, M. & Collins, M. J. Collagen survival and its use for species identification in Holocene-lower Pleistocene bone fragments from British archaeological and paleontological sites. *Antiqua* **1**, e1 (2011).
48. Race, G. J. et al. Ancient Nubian human bone: a chemical and ultrastructural characterization including collagen. *Am. J. Phys. Anthropol.* **28**, 157–162 (1968).
49. Wyckoff, R. W. G., Wagner, E., Matter, P. & Dobrenz, A. R. Collagen in fossil bone. *PNAS* **50**, 215–218 (1963).
50. Miles, C. A. & Ghelashvili, M. Polymer-in-a-Box mechanism for the thermal stabilization of collagen molecules in fibers. *Biophys. J.* **76**, 3243–3252 (1999).
51. Reznikov, N., Bilton, M., Lari, L., Stevens, M. M. & Kröger, R. Fractal-like hierarchical organization of bone begins at the nanoscale. *Science* **360**, ea02189 (2018).
52. Covington, A. D., Song, L., Suparno, O., Collins, M. J. & Koon, H. E. C. Link-Lock: the mechanism of stabilising collagen by chemical reactions. *J. Soc. Leather Technol. Chem.* **92**, 1–7 (2006).
53. Wright, L. E. & Schwarcz, H. P. Infrared and isotopic evidence for diagenesis of bone apatite at Dos Pilas, Guatemala: palaeodietary implications. *J. Archaeol. Sci.* **23**, 933–944 (1996).
54. Tamara, L., Irena, Z. P., Ivan, J. & Matija, Č. ATR-FTIR spectroscopy as a pre-screening technique for the PMI assessment and DNA preservation in human skeletal remains – A review. *Quat. Int.* **660**, 56–64 (2022).
55. Dal Sasso, G. et al. Bone diagenesis variability among multiple burial phases at Al Khiday (Sudan) investigated by ATR-FTIR spectroscopy. *Palaeogeogr. Palaeoclimatol. Palaeoecol.* **463**, 168–179 (2016).
56. Smith, C. I., Nielsen-Marsh, C. M., Jans, M. M. E. & Collins, M. J. Bone diagenesis in the European Holocene I: patterns and mechanisms. *J. Archaeol. Sci.* **34**, 1485–1493 (2007).
57. Beyer, R. M., Krapp, M. & Manica, A. High-resolution terrestrial climate, bioclimate and vegetation for the last 120,000 years. *Sci. Data* **7**, 236 (2020).
58. R. Core Team. *R: A language and environment for statistical computing* (R Foundation for statistical computing, Vienna, 2021).
59. Leonardi, M., Hallett, E. Y., Beyer, R., Krapp, M. & Manica, A. pastclim 1.2: an R package to easily access and use paleoclimatic reconstructions. *Ecography*, e06481, <https://doi.org/10.1111/ecog.06481> (2023).
60. Gilbert, M. T. P. et al. Whole-genome shotgun sequencing of mitochondria from ancient hair shafts. *Science* **317**, 1927–1930 (2007).
61. Van der Sluis, L. G. et al. Combining histology, stable isotope analysis and ZooMS collagen fingerprinting to investigate the taphonomic history and dietary behaviour of extinct giant tortoises from the Mare aux Songes deposit on Mauritius. *Palaeogeogr. Palaeoclimatol. Palaeoecol.* **416**, 80–91 (2014).
62. Peters, C. et al. Species identification of Australian marsupials using collagen fingerprinting. *R. Soc. Open Sci.* **8**, 211229 (2021).
63. Buckley, M., Cosgrove, R., Garvey, J. & Prideaux, G. J. Identifying remains of extinct kangaroos in Late Pleistocene deposits using collagen fingerprinting. *J. Quat. Sci.* **32**, 653–660 (2017).
64. Wickham, H. *ggplot2. Elegant graphics for data analysis* (Springer-Verlag, New York, 2016).
65. Peters, C. MALDI-ToF-MS spectra of Late Pleistocene fossil material from Australia for ZooMS (Version 1). Zenodo, <https://doi.org/10.5281/zenodo.7825351> (2023).

## Acknowledgements

We thank the Pibulmun Wadandi Yunungjarli people, and specifically the Webb family as Traditional Custodians in the Leeuwin-Naturaliste Region, the Wattandee and Yamatji Traditional Owners, the Barada Barna people of Bigerley, South Walker Creek, the Augusteyn family of Capricorn Caves, and the Darumbal people, for supporting our research. We are also grateful to Andrea Manica for sharing a beta version of the Pastclim R package with us, and to Simon Hickenbotham and Julie Wilson for assistance in using the Q2E R package. We would also like to thank Sandra Hebestreit for technical assistance with ZooMS extractions, and Erin Scott for technical assistance with FTIR measurements. We are also grateful to Kristine Korzow Richter for helpful discussions about the paper, and to the three anonymous reference whose thoughtful comments and suggestions have helped to improve the quality of the manuscript. This research was supported by the Max Planck Society, ARC Discovery Early Career Research Fellowships awarded to T.M. (DE150101597) and G.J.P. (DE120101533), an ARC Discovery Project awarded to G.J.P. (DP120101752), and an ERC award (Adv. 787282) awarded to M.J.C.

## Author contributions

C.P. conceived and designed the study, performed laboratory analyses, analysed data, visualisation. Y.W. performed statistical analysis, visualisation. V.V. provided stratigraphic information. J.C. provided samples. J.D. provided samples. S.H. provided samples. R.L. provided samples. T.M. provided samples. C.M. provided samples, G.R. provided samples. H.R. provided samples. M.S. provided samples. T.Z. provided samples. J.L. provided samples. G.J.P. provided samples and stratigraphic information. N.B. conceived and designed the study. M.J.C. conceived and designed the study, and analysed data. C.P., Y.W., V.V., G.J.P. and M.J.C. wrote the paper, with critical input from all authors.

## Funding

Open Access funding enabled and organized by Projekt DEAL.

## Competing interests

The authors declare no competing interests.

## Additional information

**Supplementary information** The online version contains supplementary material available at <https://doi.org/10.1038/s43247-023-01114-8>.

**Correspondence** and requests for materials should be addressed to Carli Peters.

**Peer review information** *Communications Earth & Environment* thanks Virginia L. Harvey and the other, anonymous, reviewer(s) for their contribution to the peer review of this work. Primary Handling Editor: Aliénor Lavergne. A peer review file is available.

**Reprints and permission information** is available at <http://www.nature.com/reprints>

**Publisher's note** Springer Nature remains neutral with regard to jurisdictional claims in published maps and institutional affiliations.



**Open Access** This article is licensed under a Creative Commons Attribution 4.0 International License, which permits use, sharing,

adaptation, distribution and reproduction in any medium or format, as long as you give appropriate credit to the original author(s) and the source, provide a link to the Creative Commons license, and indicate if changes were made. The images or other third party material in this article are included in the article's Creative Commons license, unless indicated otherwise in a credit line to the material. If material is not included in the article's Creative Commons license and your intended use is not permitted by statutory regulation or exceeds the permitted use, you will need to obtain permission directly from the copyright holder. To view a copy of this license, visit <http://creativecommons.org/licenses/by/4.0/>.

© The Author(s) 2023